THE FASEB JOURNAL • RESEARCH • www.fasebj.org

Mitochondrial structure and function are not different between nonfailing donor and end-stage failing human hearts

Katherine M. Holzem,* Kalyan C. Vinnakota,† Vinod K. Ravikumar,* Eli J. Madden,* Gregory A. Ewald,‡ Krikor Dikranian,‡ Daniel A. Beard,† and Igor R. Efimov*,§,1

‡Washington University School of Medicine, and *Department of Biomedical Engineering, Washington University in St. Louis, St. Louis, Missouri, USA; †Department of Molecular and Integrative Physiology, University of Michigan, Ann Arbor, Michigan, USA; and §George Washington University, Washington, D.C., USA

ABSTRACT: During human heart failure, the balance of cardiac energy use switches from predominantly fatty acids (FAs) to glucose. We hypothesized that this substrate shift was the result of mitochondrial degeneration; therefore, we examined mitochondrial oxidation and ultrastructure in the failing human heart by using respirometry, transmission electron microscopy, and gene expression studies of demographically matched donor and failing human heart left ventricular (LV) tissues. Surprisingly, respiratory capacities for failing LV isolated mitochondria ($n = 9$) were not significantly diminished compared with donor LV isolated mitochondria ($n = 7$) for glycolysis (pyruvate + malate)- or FA (palmitoylcarnitine)-derived substrates, and mitochondrial densities, assessed *via* citrate synthase activity, were consistent between groups. Transmission electron microscopy images also showed no ultrastructural remodeling for failing *vs.* donor mitochondria; however, the fraction of lipid droplets (LDs) in direct contact with a mitochondrion was reduced, and the average distance between an LD and its nearest neighboring mitochondrion was increased. Analysis of FA processing gene expression between donor and failing LVs revealed 0.64-fold reduced transcript levels for the mitochondrial-LD tether, perilipin 5, in the failing myocardium ($P = 0.003$). Thus, reduced FA use in heart failure may result from improper delivery, potentially *via* decreased perilipin 5 expression and mitochondrial-LD tethering, and not from intrinsic mitochondrial dysfunction.—Holzem, K. M., Vinnakota, K. C., Ravikumar, V. K., Madden, E. J., Ewald, G. A., Dikranian, K., Beard, D. A., Efimov, I. R. Mitochondrial structure and function are not different between nonfailing donor and end-stage failing human hearts. FASEB J. 30, 2698–2707 (2016). www.fasebj.org

KEY WORDS: oxidative respiration · electron microscopy · energy substrate · lipid droplet · perilipin 5

Heart failure (HF) is the end stage of many cardiovascular diseases, in which hypertrophic remodeling no longer meets cardiac output demand. The burden of HF has reached epidemic proportions, with >20 million people affected worldwide (1). During the progression to HF, the heart switches energy substrate use from preferential utilization of fatty acids (FAs) to greater glucose consumption (2). Although glucose is a more efficient oxidative substrate for ATP synthesis, the heart is not able to compensate for ATP demand, and this state of limited energy supply may contribute to disease pathogenesis (3, 4). In addition, mitochondrial respiratory dysfunction has been reported in animal models of HF (5, 6), but respiratory studies in the failing human heart have yielded inconsistent results (7–11). Mitochondrial degeneration has also been presumed from cardiomyopathic specimen ultrastructure, though these studies were performed without corresponding donor specimens (12–17). Nevertheless, augmenting mitochondrial function has been considered as a therapeutic strategy for HF (18, 19).

We hypothesized that asymmetrically impaired mitochondrial respiratory capacity contributes to substrate utilization shift in the failing human heart; therefore, we anticipated reductions in oxidative respiration, with a greater defect in FA *vs.* glycolytic substrate respiratory capacity. We assessed respiration rates for the glycolysis-derived substrate, pyruvate + malate (PM),

ABBREVIATIONS: ATGL, adipose triglyceride lipase; BMI, body mass index; CD, cluster of differentiation; CS, citrate synthase; FA, fatty acid; HF, heart failure; ICM, ischemic cardiomyopathy; LD, lipid droplet; LPL, lipoprotein lipase; LV, left ventricle; NICM, nonischemic cardiomyopathy; OR, operating room; PC, palmitoylcarnitine; PDK4, pyruvate dehydrogenase kinase 4; PLIN5, perilipin 5; PM, pyruvate + malate; PPAR, peroxisome proliferator-activated receptor; TEM, transmission electron microscopy

[1] Correspondence: Department of Biomedical Engineering, George Washington University, 5000C Science & Engineering Hall, 800 22nd St. NW, Washington, D.C. 20052, USA. E-mail: efimov@gwu.edu

doi: 10.1096/fj.201500118R
This article includes supplemental data. Please visit *http://www.fasebj.org* to obtain this information.

and FA-derived substrate, palmitoylcarnitine (PC), in isolated mitochondria from both human donor and failing left ventricular (LV) tissue. We also predicted that respiratory impairment in failing heart mitochondria would be associated with mitochondrial structural deterioration, assessed by transmission electron microscopy (TEM).

Contrary to our expectations, we found neither functional nor structural alterations in failing heart mitochondria. Thus, we proceeded to investigate energy substrate handling preceding mitochondrial use. By using TEM image analysis, we quantified mitochondrial–lipid droplet (LD) coupling and found that the fraction of LDs in direct contact with mitochondria was reduced in failure. In addition, we examined the expression of several genes that are important for FA processing and found that expression of perilipin 5 (*PLIN5*), which regulates LD tethering to mitochondria, is reduced in HF. Taken together, our findings suggest that metabolic remodeling of energy substrate utilization in human HF is not the result of intrinsic mitochondrial functional or structural degeneration. Instead, our ultrastructural and gene expression data support the theory that FA delivery to mitochondria may be impaired. These findings have important implications for therapeutic strategies to support metabolism in failing human myocardium.

MATERIALS AND METHODS

Human heart recovery and clinical data

All studies using human heart tissue have been approved by the institutional review board at Washington University School of Medicine. We recovered donor human hearts that were rejected for transplantation from the Mid-America Transplant Services (St. Louis, MO, USA), and end-stage failing hearts from transplantation recipients at Barnes-Jewish Hospital (St. Louis, MO, USA). In total, all studies (respiration, TEM, and gene expression) used 34 donor and 39 failing hearts. All hearts were explanted by a cardiothoracic surgeon and were rapidly transferred to a member of the research team in the operating room (OR). Coronary artery perfusion with ice-cold cardioplegic solution (110 mM NaCl, 1.2 mM $CaCl_2$, 16.0 mM KCl, 16.0 mM $MgCl_2$, and 10.0 $NaHCO_3$) was used to arrest hearts. Hearts were then packed in a cooler with cold cardioplegic solution to be transported to the laboratory (with a total time from heart excision to laboratory of ~20 min). After arrival, hearts were unpacked and placed in a tray with additional ice-cold cardioplegic solution for dissection. Before mitochondrial isolation, LV tissue was rapidly collected and preserved in RNA later (Sigma-Aldrich, St. Louis, MO, USA) for mRNA or flash-frozen in liquid nitrogen for enzymatic analysis. Tissue specimens for mitochondrial isolation were then dissected within 10 min from heart unpacking.

Clinical data for donor hearts were collected from Mid-America Transplant Services consent packets. Measurements of donor heart cardiovascular disease and function were obtained from clinical assessments that were conducted while evaluating the organ for donation, such as echocardiograms, coronary angiographs, and electrocardiograms. Failing heart clinical information was provided by the Translational Cardiovascular Biobank & Repository at Washington University School of Medicine, which were procured from the Barnes-Jewish Hospital electronic medical record and provided to the laboratory in a deidentified manner (**Table 1** and Supplemental Unit 1).

Mitochondrial isolation and respiration measurements

All reagents and tools for mitochondrial isolation were prepared before attending the OR for recovery. During heart dissection, a transmural LV specimen ~2–4 g was dissected from the anterior free wall (**Fig. 1*A***) and epicardial fat was excised. Tissue was then finely minced and homogenized at 4°C in a buffer that contained 200 mM mannitol, 50 mM sucrose, 5 mM KH_2PO_4, 5 mM MOPS, 1 mM EGTA, and 0.1% bovine serum albumin (pH 7.15), with 5 U/ml *Bacillus licheniformis* protease. Mitochondria were isolated through differential centrifugation, as previously described (20), and protein was quantified by bicinchoninic acid assay (Thermo Fisher Scientific Life Sciences, Waltham, MA, USA). Respiration measurements were conducted by using an Oxygraph-O2k high-resolution respirometer (Oroboros, Innsbruck, Austria) in buffer that contained 130 mM KCl, 2.5 mM K_2HPO_4, 20 mM MOPS, 1 mM EGTA, and 0.1% bovine serum albumin (pH 7.15). For our respiration protocol (Fig. 1*B*), we first injected 0.1 mg protein from the mitochondrial sample. After 70 s, substrate was added, with either PM (10 mM/2 mM) or PC (25 μM) to determine S2 respiration before ADP addition. At 110 s after substrate injection, ADP (350 μM) was added to establish S3 respiration, and the experiment was continued through to S4.

Mitochondrial enzyme activity measurement

Citrate synthase (CS) enzymatic activities were measured by spectrophotometry, and specific activities were measured during the linear phase with the changing absorbance (λ, 232 nm) of the reaction product between CoA-SH and 2-nitrobenzoic acid (protocol distributed by Oroboros). To normalize respiration data, all enzyme assays were conducted by using samples from the same hearts from which respiration data were collected.

TEM sample preparation and imaging

Specimens were dissected surrounding an LV coronary artery, which was cannulated, and major leaking branches were sutured shut. Tissue was then perfused with 2% glutaraldehyde in 0.1 M sodium cacodylate. Specimens were postfixed in 1% osmium tetroxide, dehydrated, cleared in toluene, and embedded in araldite resin. Ultrathin sections (70–80 nm) were cut with an Ultracut UCT ultramicrotome (Leica Microsystems, Buffalo Grove, IL, USA) and were mounted on Formvar coated mesh grids. Sections were counterstained with saturated ethanolic uranyl acetate, followed by lead citrate.

Images were acquired on a Jeol 100B (Jeol, Tokyo, Japan) by a separate investigator, who was blinded to the donor/failing status of the specimens. Five different regions per heart were randomly selected for an overview image (×3000), and 10 nonoverlapping analysis images (×8000) were acquired from within the overview region. Images were processed by using Fiji software (*http://fiji.sc/*). All mitochondria and LDs from images were measured (totaling ~800–2500 mitochondria/heart). Distances between mitochondria and LDs were computed as euclidean distances between centroids. Average mitochondrial grayscale (0–255) pixel intensities were measured and normalized to sarcomeric pixel intensities from the same image.

TABLE 1. *Heart groups are not different with regard to key demographic characteristics*

	Demographic characteristics						
Heart group	Gender	Age (yr)	BMI (kg/m^2)	BMI category	Comorbidities	COD or Dx	EF (%)
Donor	F	59	20.6	Normal	SH (40 y)	COD: CVA	
(n = 7)	F	54	24.1	Normal	HTN; LVH; SH (40 y)	COD: CVA	
	M	27	24.5	Normal	SH (13 y)	COD: MVA	
	M	59	25.4	Overweight	HTN	COD: CVA	
	F	73	26.4	Overweight	SH (5 y)	COD: anoxia	
	M	46	27.8	Overweight	None reported	COD: CVA	
	M	60	36.7	Obese	HTN; SH (≥40 y)	COD: anoxia	
	4:3 M:F	*54.0 ± 5.4*	*26.5 ± 1.9*	*3:4, BMI < 24.9: BMI ≥ 24.9*	*CV: 3 HTN; 1 LVH; 5 SH*	*COD: 2 anoxia; 4 CVA; 1 MVA*	
Failing	M	47	18.4	Underweight	MI/CAD; PH	Dx: ICM	30
(n = 9)	M	47	21	Normal	PH	Dx: NICM	15
	F	61	24.8	Normal	COPD; hypothyroidism; KD; OSA; PH	Dx: NICM	<20
	M	32	26	Overweight	Becker's MD; PH	Dx: NICM	NA
	F	65	28	Overweight	Myocarditis; PH	Dx: NICM	45
	F	51	28.2	Overweight	PH; SH	Dx: NICM	22
	M	63	29.4	Overweight	DM; MI/CAD; MR; PH; SH	Dx: NICM	20
	M	63	31.8	Obese	MI/CAD; PH	Dx: ICM	35
	M	43	33.2	Obese	Cirrhosis; KD; PH	Dx: NICM	50
	2:1 M:F	*52.4 ± 3.8*	*26.8 ± 1.6*	*1:2, BMI < 24.9: BMI ≥ 24.9*	*CV: 1 DM; 1 MD; 2 MI/CAD; 1 MR; 1; myocarditis; 9 PH; 2 SH*	*Dx: 2 ICM; 7 NICM*	*29.6 ± 4.5*

Of note, the comorbidity information shows a lack of dm for both heart groups, and the donor hearts demonstrate little evidence of cardiac disease. Data are presented as means ± SEM. cad, coronary artery disease; cod, cause of death; copd, chronic obstructive pulmonary disease; cva, cerebrovascular accident (stroke); dm, diabetes mellitus; dx, diagnosis; ef, ejection fraction; htn, hypertension; kd, kidney disease; lvh, lv hypertrophy; md, muscular dystrophy; mi, myocardial infarction; mr, mitral regurgitation; mva, motor vehicle accident; na, not available; osa, obstructive sleep apnea; ph, pulmonary hypertension; sh, smoking history. The text in italic is a summary of the data in table.

RNA isolation and real-time quantitative PCR

Total RNA was extracted, quantified, and reverse transcribed as previously described (21). Real-time PCR of cDNA was performed on an Applied Biosystems 7900HT sequence detector using inventoried TaqMan Gene Expression Assays for the specific gene targets analyzed (Applied Biosystems, Foster City, CA, USA). *RPL32* was used as an endogenous control because it is a stable reference gene for cardiac expression studies (22).

Statistical analysis

Statistical significance was determined by unpaired, 2-tailed Student's or Welch's t tests. Welch's t test was selected when an F test revealed unequal variance between groups. Outliers were excluded by Grubb's analysis. Data are presented as means ± SEM. A value of $P < 0.05$ was considered statistically significant.

RESULTS

Matched donor and failing human heart demographics for functional respiration measurements

Donor and failing human hearts used in our functional studies were well matched in terms of key demographic characteristics (Table 1). Of note, ages did not differ between donor and failing groups, with means of 54.0 ± 5.4 yr of age for donor and 52.4 ± 3.8 yr of age for failing groups (P = 0.81); nor were there differences in body mass indices (BMIs), with BMIs of 26.5 ± 1.9 kg/m^2 for donor and 26.8 ± 1.6 kg/m^2 for failing (P = 0.92). Comorbidity data also demonstrate a lack of diabetes mellitus or metabolic disease in either donor or failing heart groups, with only 1 failing heart patient having a history of diabetes mellitus. The ratio of males to females was similar between groups (57.1% male for donor and 66.7% male for failing). Of importance, the sample of donor hearts demonstrated little evidence of cardiac disease, with only 1 heart showing LV hypertrophy on echocardiography.

Preserved mitochondrial respiration in human HF

We conducted measurements in isolated mitochondria by the protocol outlined in **Fig. 1*A, B***. Representative O_2 concentration and flux curves with both substrates are shown in Fig. 1C. S2 respiration did not differ between donor and failing mitochondria for PM or PC substrates (**Fig. 2*A***). We also did not observe statistically significant reductions in absolute S3 respiratory capacity for failing mitochondria using PM or PC (Fig. 2*B*), with PM O_2 consumption fluxes of 195.90 ± 19.14 and 158.82 ± 9.04 nmol O_2/min/mg protein

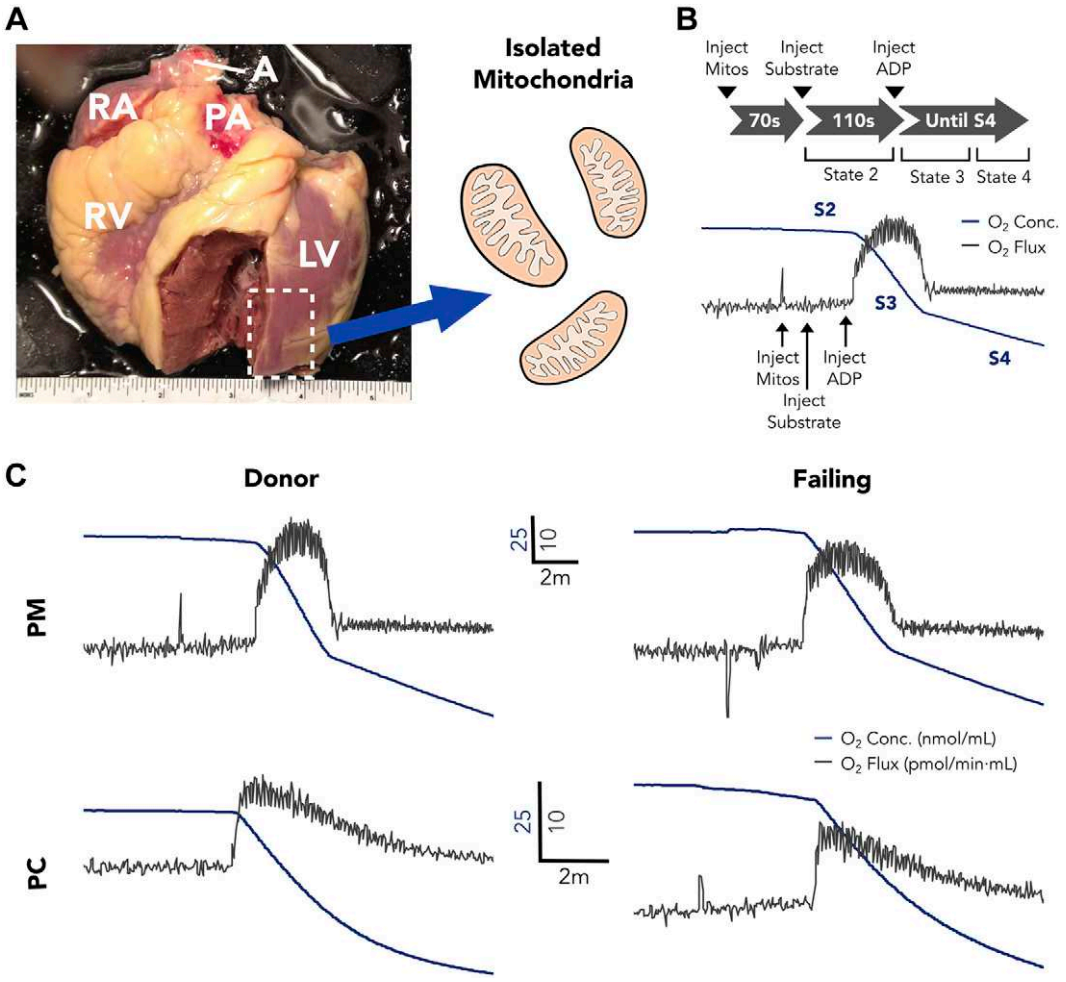

Figure 1. *A*) Representative image of a donor human heart, with dashed box indicating the mitochondrial isolation region. *B*) Mitochondrial respiration measurement protocol and example O_2 concentration and flux curves. *C*) Representative PM and PC O_2 concentration and flux curves for donor and failing hearts. A, aorta; PA, pulmonary artery; RA, right atrium; RV, right ventricle.

($P = 0.12$) and PC O_2 consumption fluxes of 122.50 ± 23.01 and 91.92 ± 14.42 nmol O_2/min/mg protein ($P = 0.19$) for donor and failing hearts, respectively. In addition, there were no differences between donor and failing mitochondria in S4 respiration for either PM or PC (Fig. 2*C*). Our summary results also demonstrate that S3/S4 or S3/S2 respiratory control ratios were not different between donor and failing heart mitochondria for either PM (S3/S4 = 6.09 ± 1.73 *vs.* 4.86 ± 0.98, $P = 0.45$, and S3/S2 = 25.4 ± 6.9 *vs.* 17.7 ± 2.2, $P = 0.24$) or PC (S3/S4 = 5.23 ± 1.32 *vs.* 4.04 ± 0.57, $P = 0.47$, and S3/S2 = 17.8 ± 7.4 *vs.* 9.1 ± 0.9, $P = 0.20$, Fig. 2*D*, *E*). To ensure consistent mitochondrial content between heart groups, we assayed CS from the same hearts used for respiration studies, and CS-specific activities were not different per g muscle tissue between donor and failing hearts (14.5 ± 2.4 *vs.* 14.7 ± 1.8 U/g tissue; $P = 0.92$; Fig. 2*F*).

No ultrastructural differences between donor and failing heart mitochondria

We proceeded to examine whether there were ultrastructural differences between donor and failing heart mitochondria. Because we recovered intact human hearts immediately upon excision in the OR, we conducted fixation by coronary perfusion (Fig. 3*A*–*C*, schematic), which enabled high-quality TEM image results. Examples of overview region images (magnification, ×3000) are displayed with nonoverlapping image regions (magnification, ×8000) used for quantification for donor hearts (Fig. 3*D*, *F*) and failing hearts (Fig. 3*G*–*I*). Representative zoomed-in images of individual mitochondria are shown from each of 4 separate donor and failing hearts (**Fig. 4*A*, *B***), which highlights that donor and failing heart mitochondria appear similar in size and demonstrate dense cristae packing. Further TEM myocardial images from each donor and failing heart used for ultrastructural analysis are shown in Supplemental Unit 2, along with the ultrastructure of example isolated mitochondria (Supplemental Unit 3).

We measured cross-sectional area for each mitochondrion and quantified cristae density by using average grayscale pixel intensities (0–255), normalized to sarcomeric pixel intensity for each image. Because we measured hundreds of mitochondria per heart, we analyzed frequency distribution data with LOWESS

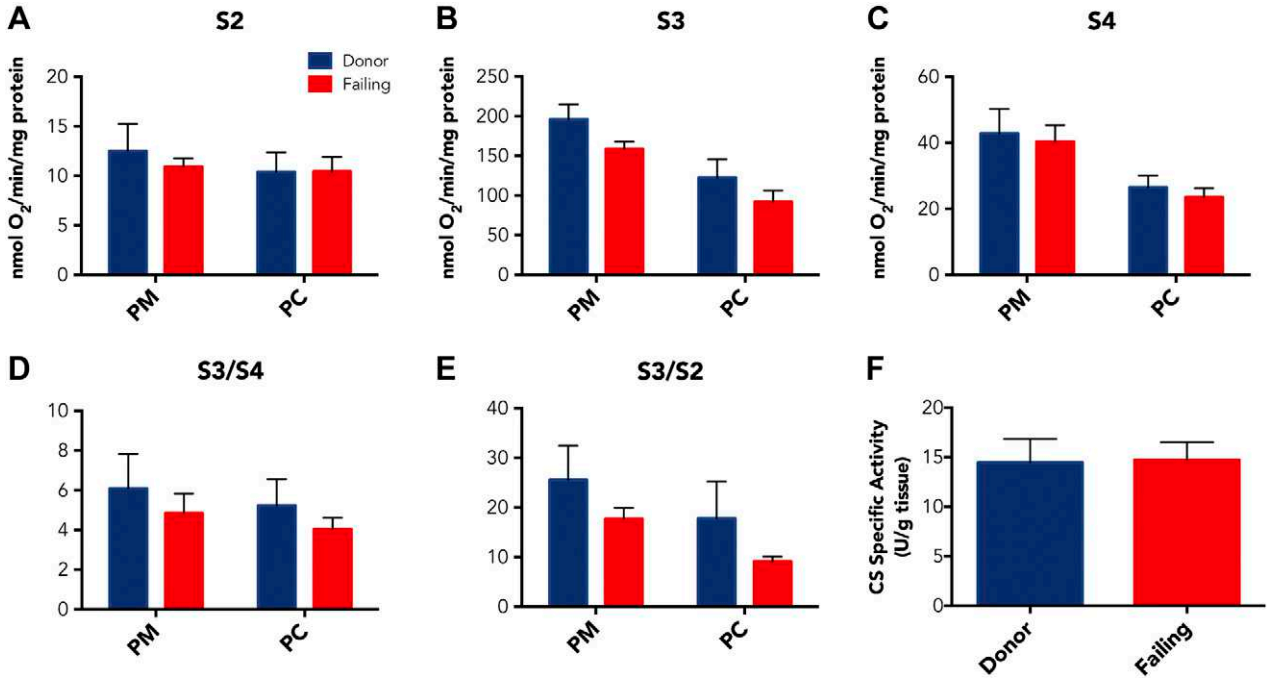

Figure 2. *A–C*) Average S2 (*A*), S3 (*B*), and S4 (*C*) respirations with PM and PC substrates for donor hearts ($n = 7$) and failing hearts ($n = 9$). *D*, *E*) S3/4 (*D*) and S3/2 (*E*) respiratory control ratios (RCRs) for donor hearts ($n = 7$) and failing hearts ($n = 9$). There were no statistically significant differences between donor and failing hearts for respiration rates or RCRs with either substrate. *F*) CS-specific activities/g muscle tissue were not different between donor hearts ($n = 7$) and failing hearts ($n = 9$). Data are expressed as means ± SEM.

regression curves. Figure 4*C–F* shows LOWESS curves of mitochondrial cross-sectional area and average pixel intensity from mitochondrial counts and percentages of total, respectively, for each donor and failing heart. When averaging results, mitochondrial area was not different between donor and failing human hearts ($2.66 \times 10^5 \pm 0.32 \times 10^5$ *vs.* $2.87 \times 10^5 \pm 0.31 \times 10^5$ nm^2; $P = 0.65$; Fig. 4*G*). In addition, average mitochondrial pixel intensities were 92.1 ± 4.7 for donor mitochondria compared with 97.6 ± 4.6 for failing heart mitochondria ($P = 0.42$; Fig. 4*H*), which indicated no differences in cristae packing within mitochondria.

Impairment of mitochondria-LD tethering and FA substrate delivery

Given the lack functional or architectural disruption within failing human heart mitochondria, we examined whether impairment in FA processing precedes mitochondrial uptake. From ultrastructural images, we assessed the physical association of mitochondria with LDs. Most LDs were in direct contact with ≥1 mitochondria in both donor and failing hearts; however, there were more isolated LDs in the failing myocardium. In **Fig. 5*A*, *B***, example TEM images show an LD in direct association with mitochondria in donor myocardium and an isolated LD in the failing heart. We counted LD-mitochondrial interactions and found the percentage of LDs in direct mitochondrial contact was reduced in failing hearts compared with donor hearts (74.1 ± 1.3 *vs.* 83.2 ± 3.7%; $P = 0.025$; Fig. 5C). In addition, average euclidean distance from an LD to its nearest neighboring mitochondrion was correspondingly increased, with distances of 833.0 ± 56.0 and 597.9 ± 51.3 nm for failing and donor hearts, respectively ($P = 0.020$; Fig. 5*D*). There were no differences in overall LD density between donor and failing hearts, though there was a trend toward increased LD density for failing hearts with nonischemic cardiomyopathy (NICM; Supplemental Unit 4).

We then examined expression of genes that are important for FA processing outside of mitochondria. We assessed transcript levels for genes that encode adipose triglyceride lipase (ATGL, encoded by *PNPLA2*), cluster of differentiation 36 (CD36, encoded by *CD36*), lipoprotein lipase (LPL, encoded by *LPL*), PLIN5 (encoded by *PLIN5*), peroxisome proliferator-activated receptor α (PPARα, encoded by *PPARA*), and PPARγ (encoded by *PPARG*). In a large sample of donor and failing human LV specimens, we identified *PLIN5* as having 0.64-fold reduced expression in failure ($P = 0.003$; Fig. 5*E*), and PLIN5 protein is known to be important for LD packaging and tethering to mitochondria (23, 24). We also found expression of *LPL* to be up-regulated by 54.3% in failing LV tissues compared with donor LV tissues ($P = 0.021$; Fig. 5*E*). None of the other FA processing genes we examined were significantly altered in failing human LV (Fig. 5*E*). Expression of *NPPA*, which encodes the atrial natriuretic peptide, was increased (3.2-fold; $P = 0.073$), and expression of *MYH6*, which encodes α-myosin heavy chain, was decreased (0.17-fold; $P = 2.4E\text{-}5$) in failing hearts compared with donor hearts, as expected (Fig. 5*F*).

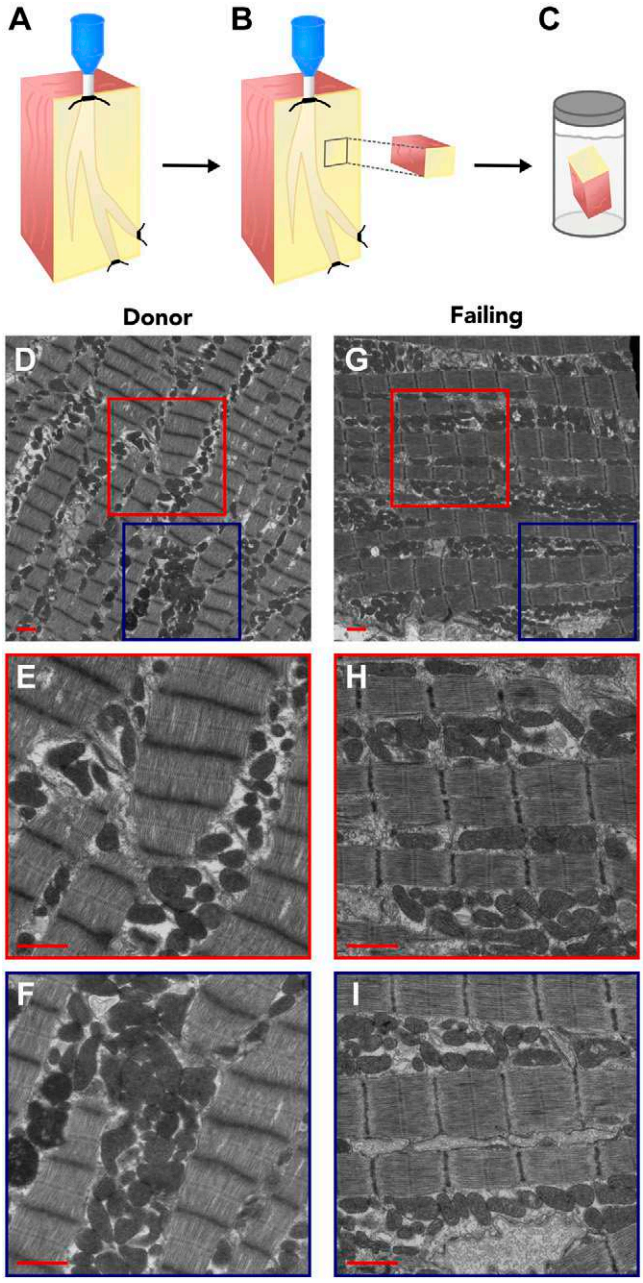

Figure 3. *A–C*) Illustrated schematic for TEM sample preservation. *A*) A portion of the LV surrounding a coronary artery was dissected and cannulated. Tissue was then perfused with fixative for optimal preservation. A small core of tissue was then excised (*B*) and stored in fixative (*C*). *D–I*) Representative electron micrographs from donor (*D–F*) and failing (*G–I*) heart muscle. *D*, *G*) Overview images; red and blue boxes outline nonoverlapping regions for donor hearts (*E*, *F*) and for failing hearts (*H*, *I*). Original magnification, ×3000 (*D*, *G*) and ×8000 (*E*, *F*, *H*, *I*) Scale bar, 1 μm.

DISCUSSION

Contrary to our hypothesis, our results demonstrate a lack of mitochondrial oxidative dysfunction for both glycolysis- and FA-derived substrates in mitochondria isolated from failing human hearts. Furthermore, TEM images of perfusion-fixed human LV myocardium reveal that mitochondria show preserved structure. Instead, our results support the theory that FA delivery to mitochondria may be impaired. Our TEM images reveal reduced LD-mitochondrial coupling and increased distances between LDs and mitochondria in failure. We also show that the transcript level for the mitochondrial-LD tether, PLIN5, is reduced in failing hearts, which may diminish the efficient coupling of mitochondria to lipid stores and impair lipolysis.

Studies that suggest mitochondrial remodeling in HF

Our findings contradict results from several animal model studies of HF, which suggest that mitochondrial respiration is impaired (5, 6). For human HF, some studies have suggested mitochondrial dysfunction solely on the basis of enzymatic activities (19, 25), whereas previous reports on mitochondrial respiration in human HF have produced inconsistent results (7, 8). In a report by Sharov *et al.* (7), PM-stimulated respiration was reduced but mitochondrial density in donor *vs.* failing hearts was not measured. In addition, although Cordero-Reyes *et al.* (8) analyzed a large number of failing heart samples, their comparison group consisted of a small number of patients with right ventricular failure, which limited their power to detect a difference between groups. Because we conducted studies with a relatively large sample of well-matched donor hearts, our investigation provides stronger evidence for lack of respiratory impairment in mitochondria from failing human hearts.

In addition, there have been several classic studies on mitochondrial architecture within the diseased human myocardium (12, 16, 26, 27). The majority of these studies were conducted by using cardiomyopathic specimens collected *via* biopsy during surgery. Fixation by diffusion into such specimens could be incomplete and may result in mitochondrial structural artifacts. Moreover, these studies were performed without corresponding donor specimens; thus, it cannot be determined whether the observed mitochondrial abnormalities were the result of true structural alterations or artifacts of preservation. In contrast, we recovered both donor and failing freshly isolated hearts, which we perfused for optimal fixation.

Age-related muscle dysfunction unrelated to mitochondrial impairment

Debate regarding the causal role of mitochondrial abnormalities in muscle dysfunction is not limited to HF. Similar contradictory studies have been published regarding human age-related muscle performance. Perhaps even more appealing than in HF, for which there is a clear extrinsic trigger for disease, is the mitochondrial theory of aging, in which progressive declines in mitochondrial function could promote muscular deterioration (28, 29). Some studies have demonstrated a relationship between impaired mitochondrial function and age in human skeletal muscle, whereas others have not found any changes with age (30–33). However, similar to our study, when large numbers of human donor and diseased specimens were analyzed, biologically and statistically significant mitochondrial differences were not apparent (34).

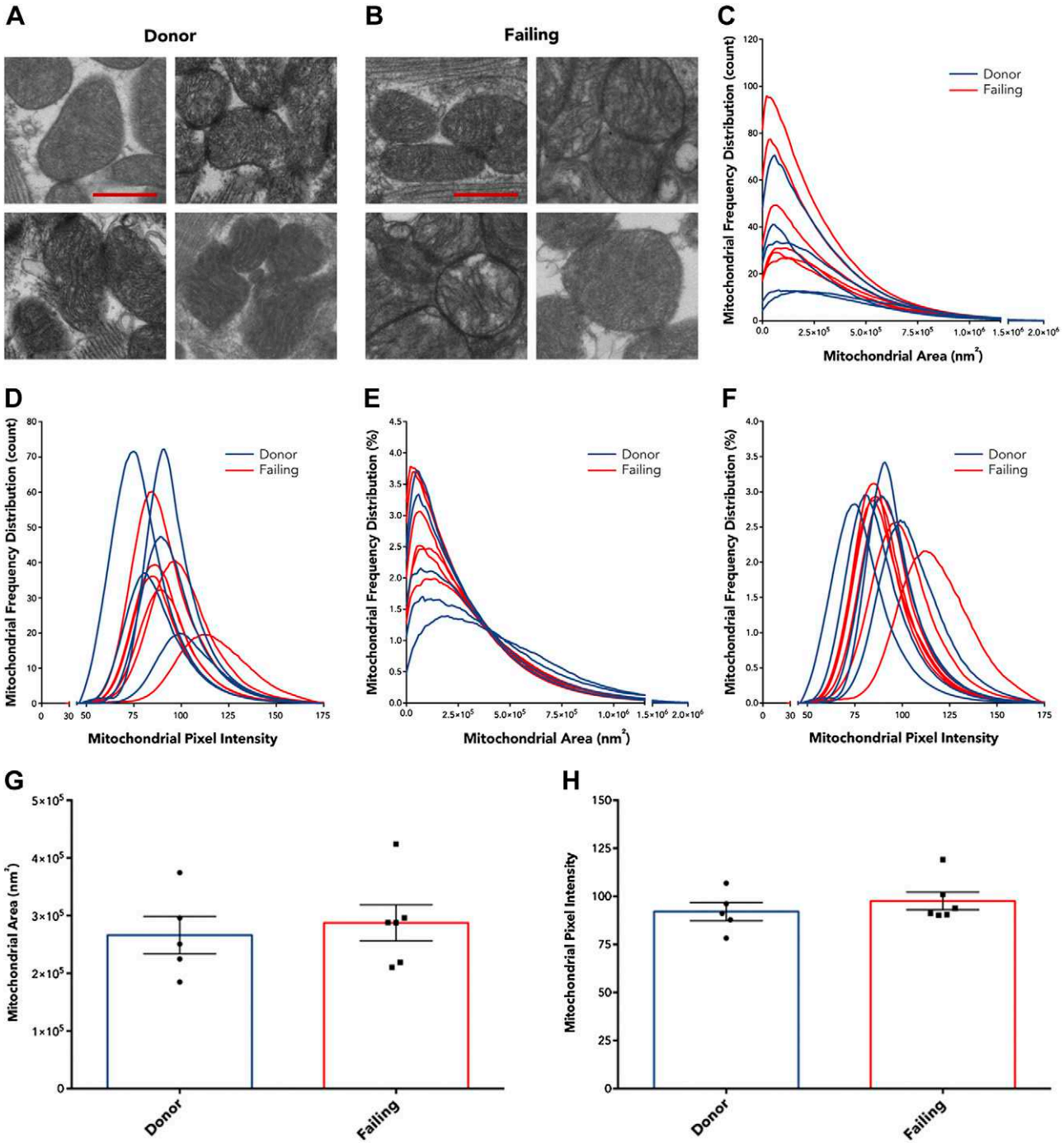

Figure 4. *A*, *B*) Representative zoomed-in images of individual mitochondria from 4 separate donor (*A*) donor and failing (*B*) hearts. *C–F*). Frequency distribution LOWESS curves for each individual heart expressed by count (*C*, *D*) and by percentage of total (*E*, *F*) for mitochondrial area (*C*, *E*) and pixel intensity (*D*, *F*). *G*, *H*) Pooled mitochondrial area (*G*) and pixel intensity (*H*), with individual heart data points, show no differences between donor hearts ($n = 5$) and failing hearts ($n = 6$). Data are expressed as means ± SEM. Scale bar, 500 nm.

Isolated mitochondria *vs.* permeabilized fibers

Mitochondrial isolation yields range from 20–40% of initial mitochondria, which potentially leads to selection bias, and respiration measurements can differ between isolated mitochondria and permeabilized fiber preparations (35, 36). These findings suggest that mitochondrial isolation leads to apparent respiratory dysfunction in diseased tissues; however, our results show no respiratory dysfunction failing isolated mitochondria, which is inconsistent with selection for dysfunctional mitochondria. Furthermore, the method of massing tissue before isolation to compute the fraction of mitochondrial recovery would be inaccurate and inappropriate for the human heart as a result of disparate amounts of fibrosis between donor and failing hearts. In human heart, the amount of fibrosis has been estimated at 6–11% in the normal heart and ≤35% in disease (37).

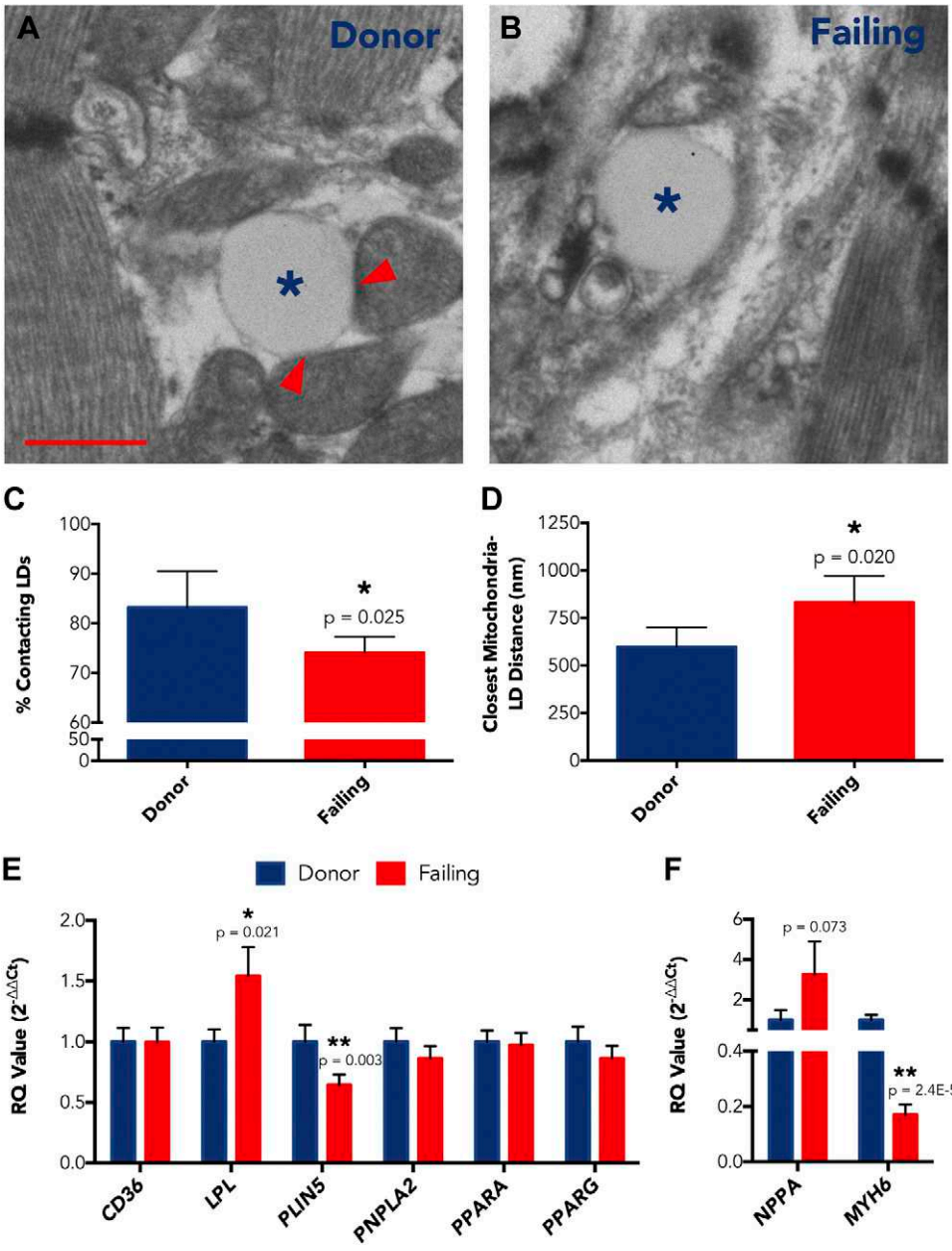

Figure 5. *A*, *B*) Representative electron micrographs showing an LD in contact with mitochondria in donor heart (*A*) and an isolated LD in failing heart (*B*). Asterisks indicate LDs; arrowheads indicate LD-mitochondrial coupling. *C*, *D*) Percent of LDs in direct mitochondrial contact (*C*) and euclidean distance between LD centroid and nearest mitochondrial centroid (*D*) for donor hearts (n = 5) and failing hearts (n = 6). *E*, *F*) Expression levels for FA processing genes (*E*) and *NPPA* and *MYH6* control genes (*F*) in donor LV (n = 26) *vs.* failing LV (n = 27). Data are expressed as means ± SEM. $*P < 0.05$; $**P < 0.01$. Scale bar, 500 nm.

FA use gene remodeling in human HF

In this study, we examined the expression of several genes that encode for proteins that are important for FA processing, including ATGL, CD36, LPL, PLIN5, PPARα, and PPARγ. Of these, we found significant down-regulation of *PLIN5* and up-regulation of *LPL*. Increased expression of LPL in the setting of HF is surprising, as it would be expected to enhance lipid uptake (38). However, altered expression of *PLIN5* in the mouse heart disrupts LD localization and cardiac substrate use (39, 40), and in rat muscle, *PLIN5* overexpression leads to better matching of FA supply to oxidative metabolism (41). Recently, PLIN5 has been shown to be regulated by PKA, with phosphorylation promoting ATGL activation and increased LD breakdown (42, 43), which indicates that *PLIN5* down-regulation may be sufficient to limit FA catabolism. PLIN5 also facilitates docking of other lipolytic proteins, which can promote cardiac dysfunction when altered (39). Thus, reduced *PLIN5* expression in human HF may disrupt LD dynamics, localization, and lipolysis.

We previously investigated energy substrate processing genes and found altered expression of *SLC27A4* and *PDK4* in human HF (21). *SLC27A4* encodes the long-chain fatty acid transport protein 4 (FATP4), which regulates cellular FA uptake (44). *SLC27A4* was down-regulated in HF, which could potentially decrease cardiac FA transport. *PDK4* encodes pyruvate dehydrogenase kinase 4 (PDK4) and its expression was increased in failing myocardium. PDK4 inhibits pyruvate dehydrogenase *via* phosphorylation, and pyruvate dehydrogenase governs the balance between cardiac glucose and FA use by bridging glycolysis with the tricarboxylic acid cycle (45). Thus, increased PDK4 might be expected to reduce glucose and enhance FA use, but PDK4 regulation could potentially be a compensatory mechanism resulting from

reduced FA utilization. However, reductions in transcript levels for FA processing proteins, including medium- and long-chain acyl-CoA dehydrogenases, CD36, and carnitine palmitoyltransferase 1, have been previously demonstrated (46, 47), although our results contradict these data. Conversely, these studies have also shown reduced transcript expression of *GLUT1* and *GLUT4*, which indicates that glucose uptake may also be inhibited in human HF. Therefore, these results suggest global metabolic suppression of both FA and glucose metabolism. Nevertheless, *PLIN5* may not be the only gene involved in reduced FA use in the failing human heart, and/or, perhaps, decreased FA processing in HF leads to altered regulation of associated genes.

Limitations

It is important to note that our nonfailing donor hearts had been rejected for transplantation and are not normal control human hearts. We have included detailed demographic data such that the degree of disease present in both heart groups can be considered with the interpretation of our results. Although the presence of comorbid disease in our donor group is a limitation of our study, this is the only means by which we can investigate pathophysiology in *ex vivo* human tissue. For obvious ethical reasons, we simply cannot use normal human heart tissue for experiment; however, we have used the best possible nonfailing human hearts available to compare with failing hearts. Thus, our central experimental comparison is that of nonfailing donor hearts without dysfunction to end-stage failing hearts with severe cardiac dysfunction, and not that of normal *vs.* failing hearts. Certainly, this distinction is important by comparison to animal model investigations, in which normal control hearts are compared with failing hearts. The lack of differences we demonstrate between donor and failing hearts, to some degree, may be related to greater similarity between these groups relative to the comparison between normal and failing animal hearts.

In addition, although interesting work has been published on differences in mitochondrial biogenesis in ischemic *vs.* dilated failing hearts (19), we cannot draw ischemic cardiomyopathy (ICM)/NICM etiology-specific conclusions in our study. We had only 2 hearts each for respiration and electron micrographic experiments with a primary diagnosis of ICM; therefore, we cannot statistically compare these with the remaining NICM hearts, and our functional and morphologic analyses are likely more reflective of NICM than of ICM. In addition, alterations in lipid metabolism have been well documented in cases of cardiomyopathy associated with diabetes/obesity, but little is known about the role of lipids in nondiabetic, nonobesity-related cardiomyopathy (48). However, previously published work suggests that cardiac FA storage and use may differ in patients with HF who have elevated BMI or who are diabetic (46, 49); thus, our TEM studies may be impacted by factors other than HF.

CONCLUSIONS

To our knowledge, this is the first detailed study to compare both the function and morphology of mitochondria between nonfailing donor hearts and failing human hearts, and we have demonstrated that mitochondrial respiration and ultrastructure are surprisingly preserved in end-stage human HF. Thus, our work strongly suggests that mitochondria are not the cause of metabolic remodeling in human failing myocardium. Instead, we find reductions in the percent of LDs directly contacting mitochondria and in transcript levels for *PLIN5*, which suggest that FA use preceding the mitochondria may be impaired. We therefore conclude that reduced consumption of FAs for fuel and relatively greater glucose consumption occurs from remodeling processes extrinsic to the mitochondria. Thus, improved therapeutic strategies to support energy substrate metabolism in HF should focus less on unimpaired mitochondrial respiratory function and more on earlier stages of FA processing and delivery. FJ

The authors thank the surgical teams at Barnes-Jewish Hospital and Mid-America Transplant Services for their assistance with human heart procurement, most notably Drs. Scott Silvestry and Michael Pasque. The authors recognize the Translational Cardiovascular Biobank and Repository (Washington University in St. Louis), which is supported by the U.S. National Institutes of Health (NIH) Clinical and Translational Science Awards program (Grant UL1TR000448), and the Richard J. Wilkinson Trust, for the provision of patient records. The authors also recognize the Nutrition and Obesity Research Center for the use of their Orobos Oxygraph-O2k, and the laboratories of Jan Bieschke and Jeanne Nerbonne for the use of the NanoPhotometer P-Class and 7900HT equipment, respectively. The authors thank Marlyn Levy (Washington University Department of Cell Biology and Physiology Electron Microscopy Facility) for processing samples. This work was supported by the NIH National Heart, Lung, and Blood Institute [Grants R01HL114395 and F30HL114310 (to K.H.)], and by the American Heart Association [Grant 12PRE12050315 (to K.H.)]. The authors declare no conflicts of interest.

REFERENCES

1. Roger, V. L. (2013) Epidemiology of heart failure. *Circ. Res.* **113**, 646–659
2. Neubauer, S. (2007) The failing heart–an engine out of fuel. *N. Engl. J. Med.* **356**, 1140–1151
3. Marín-García, J., and Goldenthal, M. J. (2008) Mitochondrial centrality in heart failure. *Heart Fail. Rev.* **13**, 137–150
4. Ingwall, J. S. (2009) Energy metabolism in heart failure and remodelling. *Cardiovasc. Res.* **81**, 412–419
5. Rosca, M. G., Vazquez, E. J., Kerner, J., Parland, W., Chandler, M. P., Stanley, W., Sabbah, H. N., and Hoppel, C. L. (2008) Cardiac mitochondria in heart failure: decrease in respirasomes and oxidative phosphorylation. *Cardiovasc. Res.* **80**, 30–39
6. Sharov, V. G., Goussev, A., Lesch, M., Goldstein, S., and Sabbah, H. N. (1998) Abnormal mitochondrial function in myocardium of dogs with chronic heart failure. *J. Mol. Cell. Cardiol.* **30**, 1757–1762
7. Sharov, V. G., Todor, A. V., Silverman, N., Goldstein, S., and Sabbah, H. N. (2000) Abnormal mitochondrial respiration in failed human myocardium. *J. Mol. Cell. Cardiol.* **32**, 2361–2367
8. Cordero-Reyes, A. M., Gupte, A. A., Youker, K. A., Loebe, M., Hsueh, W. A., Torre-Amione, G., Taegtmeyer, H., and Hamilton, D. J. (2014) Freshly isolated mitochondria from failing human hearts exhibit preserved respiratory function. *J. Mol. Cell. Cardiol.* **68**, 98–105
9. Chidsey, C. A., Weinbach, E. C., Pool, P. E., and Morrow, A. G. (1966) Biochemical studies of energy production in the failing human heart. *J. Clin. Invest.* **45**, 40–50
10. Lemieux, H., Semsroth, S., Antretter, H., Höfer, D., and Gnaiger, E. (2011) Mitochondrial respiratory control and early defects of oxidative phosphorylation in the failing human heart. *Int. J. Biochem. Cell Biol.* **43**, 1729–1738
11. Stride, N., Larsen, S., Hey-Mogensen, M., Sander, K., Lund, J. T., Gustafsson, F., Køber, L., and Dela, F. (2013) Decreased mitochondrial

oxidative phosphorylation capacity in the human heart with left ventricular systolic dysfunction. *Eur. J. Heart Fail.* **15**, 150–157
12. Sekiguchi, M. (1974) Electron microscopical observations of the myocardium in patients with idiopathic cardiomyopathy using endomyocardial biopsy. *J. Mol. Cell. Cardiol.* **6**, 111–122
13. Smith, M. N., and Klima, M. (1976) Incidence of intermembrane alterations in human heart mitochondria: a preliminary ultrastructural study. *Am. Heart J.* **91**, 563–570
14. Zick, M., Rabl, R., and Reichert, A. S. (2009) Cristae formation-linking ultrastructure and function of mitochondria. *Biochim. Biophys. Acta* **1793**, 5–19
15. Ferrans, V. J., Morrow, A. G., and Roberts, W. C. (1972) Myocardial ultrastructure in idiopathic hypertrophic subaortic stenosis. A study of operatively excised left ventricular outflow tract muscle in 14 patients. *Circulation* **45**, 769–792
16. Maron, B. J., Ferrans, V. J., and Roberts, W. C. (1975) Ultrastructural features of degenerated cardiac muscle cells in patients with cardiac hypertrophy. *Am. J. Pathol.* **79**, 387–434
17. Sabbah, H. N., Sharov, V., Riddle, J. M., Kono, T., Lesch, M., and Goldstein, S. (1992) Mitochondrial abnormalities in myocardium of dogs with chronic heart failure. *J. Mol. Cell. Cardiol.* **24**, 1333–1347
18. Fillmore, N., and Lopaschuk, G. D. (2013) Targeting mitochondrial oxidative metabolism as an approach to treat heart failure. *Biochim. Biophys. Acta* **1833**, 857–865
19. Ahuja, P., Wanagat, J., Wang, Z., Wang, Y., Liem, D. A., Ping, P., Antoshechkin, I. A., Margulies, K. B., and Maclellan, W. R. (2013) Divergent mitochondrial biogenesis responses in human cardiomyopathy. *Circulation* **127**, 1957–1967
20. Smith, J. R., Matus, I. R., Beard, D. A., and Greene, A. S. (2008) Differential expression of cardiac mitochondrial proteins. *Proteomics* **8**, 446–462
21. Ng, F. S., Holzem, K. M., Koppel, A. C., Janks, D., Gordon, F., Wit, A. L., Peters, N. S., and Efimov, I. R. (2014) Adverse remodeling of the electrophysiological response to ischemia-reperfusion in human heart failure is associated with remodeling of metabolic gene expression. *Circ Arrhythm Electrophysiol* **7**, 875–882
22. Brattelid, T., Winer, L. H., Levy, F. O., Liestøl, K., Sejersted, O. M., and Andersson, K. B. (2010) Reference gene alternatives to Gapdh in rodent and human heart failure gene expression studies. *BMC Mol. Biol.* **11**, 22
23. Wang, H., Sreenivasan, U., Hu, H., Saladino, A., Polster, B. M., Lund, L. M., Gong, D. W., Stanley, W. C., and Sztalryd, C. (2011) Perilipin 5, a lipid droplet-associated protein, provides physical and metabolic linkage to mitochondria. *J. Lipid Res.* **52**, 2159–2168
24. Wang, H., and Sztalryd, C. (2011) Oxidative tissue: perilipin 5 links storage with the furnace. *Trends Endocrinol. Metab.* **22**, 197–203
25. Jarreta, D., Orús, J., Barrientos, A., Miró, O., Roig, E., Heras, M., Moraes, C. T., Cardellach, F., and Casademont, J. (2000) Mitochondrial function in heart muscle from patients with idiopathic dilated cardiomyopathy. *Cardiovasc. Res.* **45**, 860–865
26. Leyton, R. A., and Sonnenblick, E. H. (1969) The ultrastructure of the failing heart. *Am. J. Med. Sci.* **258**, 304–327
27. Maron, B. J., and Ferrans, V. J. (1978) Ultrastructural features of hypertrophied human ventricular myocardium. *Prog. Cardiovasc. Dis.* **21**, 207–238
28. Anson, R. M., and Bohr, V. A. (2000) Mitochondria, oxidative DNA damage, and aging. *J. Am. Aging Assoc.* **23**, 199–218
29. Lenaz, G. (1998) Role of mitochondria in oxidative stress and ageing. *Biochim. Biophys. Acta* **1366**, 53–67
30. Barrientos, A., Casademont, J., Rötig, A., Miró, O., Urbano-Márquez, A., Rustin, P., and Cardellach, F. (1996) Absence of relationship between the level of electron transport chain activities and aging in human skeletal muscle. *Biochem. Biophys. Res. Commun.* **229**, 536–539
31. Chretien, D., Gallego, J., Barrientos, A., Casademont, J., Cardellach, F., Munnich, A., Rötig, A., and Rustin, P. (1998) Biochemical parameters for the diagnosis of mitochondrial respiratory chain deficiency in humans, and their lack of age-related changes. *Biochem. J.* **329**, 249–254
32. Boffoli, D., Scacco, S. C., Vergari, R., Solarino, G., Santacroce, G., and Papa, S. (1994) Decline with age of the respiratory chain activity in human skeletal muscle. *Biochim. Biophys. Acta* **1226**, 73–82
33. Trounce, I., Byrne, E., and Marzuki, S. (1989) Decline in skeletal muscle mitochondrial respiratory chain function: possible factor in ageing. *Lancet* **1**, 637–639
34. Rasmussen, U. F., Krustrup, P., Kjaer, M., and Rasmussen, H. N. (2003) Experimental evidence against the mitochondrial theory of aging. A study of isolated human skeletal muscle mitochondria. *Exp. Gerontol.* **38**, 877–886
35. Picard, M., Ritchie, D., Wright, K. J., Romestaing, C., Thomas, M. M., Rowan, S. L., Taivassalo, T., and Hepple, R. T. (2010) Mitochondrial functional impairment with aging is exaggerated in isolated mitochondria compared to permeabilized myofibers. *Aging Cell* **9**, 1032–1046
36. Picard, M., Taivassalo, T., Ritchie, D., Wright, K. J., Thomas, M. M., Romestaing, C., and Hepple, R. T. (2011) Mitochondrial structure and function are disrupted by standard isolation methods. *PLoS One* **6**, e18317
37. Rossi, M. A. (2001) Connective tissue skeleton in the normal left ventricle and in hypertensive left ventricular hypertrophy and chronic chagasic myocarditis. *Med. Sci. Monit.* **7**, 820–832
38. Yagyu, H., Chen, G., Yokoyama, M., Hirata, K., Augustus, A., Kako, Y., Seo, T., Hu, Y., Lutz, E. P., Merkel, M., Bensadoun, A., Homma, S., and Goldberg, I. J. (2003) Lipoprotein lipase (LpL) on the surface of cardiomyocytes increases lipid uptake and produces a cardiomyopathy. *J. Clin. Invest.* **111**, 419–426
39. Wang, H., Sreenivasan, U., Gong, D. W., O'Connell, K. A., Dabkowski, E. R., Hecker, P. A., Ionica, N., Konig, M., Mahurkar, A., Sun, Y., Stanley, W. C., and Sztalryd, C. (2013) Cardiomyocyte-specific perilipin 5 overexpression leads to myocardial steatosis and modest cardiac dysfunction. *J. Lipid Res.* **54**, 953–965
40. Kuramoto, K., Okamura, T., Yamaguchi, T., Nakamura, T. Y., Wakabayashi, S., Morinaga, H., Nomura, M., Yanase, T., Otsu, K., Usuda, N., Matsumura, S., Inoue, K., Fushiki, T., Kojima, Y., Hashimoto, T., Sakai, F., Hirose, F., and Osumi, T. (2012) Perilipin 5, a lipid droplet-binding protein, protects heart from oxidative burden by sequestering fatty acid from excessive oxidation. *J. Biol. Chem.* **287**, 23852–23863
41. Bosma, M., Minnaard, R., Sparks, L. M., Schaart, G., Losen, M., de Baets, M. H., Duimel, H., Kersten, S., Bickel, P. E., Schrauwen, P., and Hesselink, M. K. (2012) The lipid droplet coat protein perilipin 5 also localizes to muscle mitochondria. *Histochem. Cell Biol.* **137**, 205–216
42. Pollak, N. M., Jaeger, D., Kolleritsch, S., Zimmermann, R., Zechner, R., Lass, A., and Haemmerle, G. (2015) The interplay of protein kinase A and perilipin 5 regulates cardiac lipolysis. *J. Biol. Chem.* **290**, 1295–1306
43. Mason, R. R., and Watt, M. J. (2015) Unraveling the roles of PLIN5: linking cell biology to physiology. *Trends Endocrinol. Metab.* **26**, 144–152
44. Milger, K., Herrmann, T., Becker, C., Gotthardt, D., Zickwolf, J., Ehehalt, R., Watkins, P. A., Stremmel, W., and Füllekrug, J. (2006) Cellular uptake of fatty acids driven by the ER-localized acyl-CoA synthetase FATP4. *J. Cell Sci.* **119**, 4678–4688
45. Stanley, W. C., Recchia, F. A., and Lopaschuk, G. D. (2005) Myocardial substrate metabolism in the normal and failing heart. *Physiol. Rev.* **85**, 1093–1129
46. Chokshi, A., Drosatos, K., Cheema, F. H., Ji, R., Khawaja, T., Yu, S., Kato, T., Khan, R., Takayama, H., Knöll, R., Milting, H., Chung, C. S., Jorde, U., Naka, Y., Mancini, D. M., Goldberg, I. J., and Schulze, P. C. (2012) Ventricular assist device implantation corrects myocardial lipotoxicity, reverses insulin resistance, and normalizes cardiac metabolism in patients with advanced heart failure. *Circulation* **125**, 2844–2853
47. Razeghi, P., Young, M. E., Alcorn, J. L., Moravec, C. S., Frazier, O. H., and Taegtmeyer, H. (2001) Metabolic gene expression in fetal and failing human heart. *Circulation* **104**, 2923–2931
48. Goldberg, I. J., Trent, C. M., and Schulze, P. C. (2012) Lipid metabolism and toxicity in the heart. *Cell Metab.* **15**, 805–812
49. Sharma, S., Adrogue, J. V., Golfman, L., Uray, I., Lemm, J., Youker, K., Noon, G. P., Frazier, O. H., and Taegtmeyer, H. (2004) Intramyocardial lipid accumulation in the failing human heart resembles the lipotoxic rat heart. *FASEB J.* **18**, 1692–1700

Received for publication October 23, 2015.
Accepted for publication April 5, 2016.